THE INFLUENCE OF INCOHERENT PARTICLES ON FATIGUE CRACK PROPAGATION UNDER VARIABLE AMPLITUDE LOADING IN HIGH-STRENGTH ALUMINUM ALLOYS

K. Schulte*

In high-strength aluminum alloys the fatigue crack propagation rate under constant amplitude loading conditions decreases with decreasing volume fraction of incoherent particles. However, under high-low loading sequences, where retardation in fatigue crack propagation occurs, the purer the alloy, the lower the retardation behavior. The volume fraction, the distribution and the size of the incoherent particles are the reason for the differences in retardation. This will be explained.

INTRODUCTION

In recent publications it was shown that the fatigue crack propagation behavior observed under constant amplitude loading conditions is not suitable to quantitatively describe the crack propagation behavior under service loads (variable amplitude loading conditions)(1-3). Newer alloys; e.g. Al 7475 and Al 7050, have a significant improvement in fracture toughness over the older alloys, especially Al 7075 (4) because of an increased purity (a lower content of iron and silicone). This leads also to an improvement in the fatigue crack propagation behavior under constant amplitude loading conditions. Fig. 1 shows a comparison between the constant amplitude fatigue crack propagation behavior of Al 7075-T6 and Al 7475-T761. However, in a fatigue crack propagation test under service loads, the superior behavior of Al 7475 vanishes (2,5) especially for load histories with infrequent peak loads. Fig. 2 shows the fatigue crack propagation behavior of Al 7475-T761 and Al 7075-T6 for a Mini-TWIST (6) load sequence. It can be seen, that after the flight type A (which is the severest flight in the load history), the alloy Al 7075 shows a superior behavior over Al 7475. With increasing crack length due to flight type A load history, this superior behavior becomes even more favorable. After flight type A, retardation in fatigue crack propagation occurs, and this is more obvious in Al 7075 than in Al 7475. The main distinction between these two alloys is the lower content of iron and silicon in Al 7475, so microstructural differences can be the reason for the observed variations in fatigue crack propagation.

Experimental Program

To further investigate the microstructural influence in addition to the technical alloys (which already exhibit a different content of constituent particles) a pure AL X-7075 alloy, which has nearly no particles, was chosen. In order to avoid environmental influences, the tests were performed

*DFVLR, Inst. für Werkstoff-Forschung, 5000 Köln 90, FRG

in vacuum. Due to a homogenization for 1h at 465°C, the alloys received the same subsequent heat treatment of 24h at 100°C; and they all were in an under-aged condition. The yield strength was about 420 N/mn^2 and the strain to fracture was about 0.33 (compare Table 1). For constant amplitude loading tests the alloy Al X-7075 had the best and Al 7075 the worst fatigue crack propagation behavior over the entire Δk-range (Fig. 3). This is due to the fact that Al 7075 contains iron and silicon, which both form large incoherent particles (diameter about 10-50 µm), as well as chromium which forms small incoherent particles (diameter about 0.5 µm). The chemical composition of the alloys is shown in Table 1. Al 7075 and Al 7475 show a slip-band type fatigue crack propagation mechanism at low da/dN- and Δk-rates. With increasing crack propagation rate, a transition to fracture by void coalescence occurs. This because the incoherent particles break or the particle matrix interface fails with increasing plastic deformations ahead of the crack tip, due to the higher Δk-values. Voids are formed and coalesce during fatigue crack propagation and form the dimples seen in the inserted scanning electronic micrographs in Fig. 3. Al X-7075 which contains no iron, silicone and chromium has a fatigue crack propagation mechanism along slip bands over the entire da/dN- and Δk-range, which leads to the superior fatigue crack propagation behavior under constant amplitude loading conditions.

Table 1 - Mechanical Properties and Chemical Composition of the Investigated Alloys

Alloy	Cu	Zn	Mg	Mn	Cr	Si	Fe
Al 7075	1,68	5,6	2,5	0,08	0,25	0,4	0,5
Al 7475	1,63	5,7	2,4	0,02	0,21	0,05	0,08
Al X-7075	1,5	5,7	2,5	-	<0,001	0,003	<0,003

Alloy	Aging Treatment	E MN/m^2	σ_y MN/m^2	ε_f	K_Q MN/m^2
Al 7075	T6	72 000	486	0,3	75
	24 h 100°C	72 000	415	0,33	74
Al 7475	T761	71 000	434	0,36	150
	24 h 100°C	71 000	420	0,36	115
Al X-7075	24 h 100°C	72 000	430	0,33	104

In a simple high-low loading sequence, which avoids a complicated superposition of crack accelerating and decelerating effects which can occur under flight simulation tests, it can be shown that the retardation in fatigue crack propagation is more pronounced in Al 7075, although the constant amplitude loading behavior is worse. The retardation is less pronounced for Al X-7075, which had the best fatigue crack propagation behavior under constant amplitude loading conditions of the three alloys investigated (Fig. 4).

Fig. 5 shows a scanning electron micrograph of the fracture surface of the Al 7075 alloy. A change in the microstructural crack propagation mechanism from the dimple type, due to void coalescence in the high loading period, to the slip band type in the low loading period can be observed. The same observation could be made for Al 7475, but for Al X-7075 no change in the mechanism could be investigated, as expected.

DISCUSSION

Al 7075, the alloy with the worst behavior under constant amplitude loading and the lowest fracture toughness (compared to Al 7475 and Al X-7075), shows the superior fatigue crack propagation behavior under flight simulation tests or high-low block loading sequences. This interesting fatigue crack propagation behavior can be explained only by the differences in the microstructure of the three alloys investigated. When all the alloys had the same heat treatment and only differed in the amount and size of incoherent particles, the results shown in Figs. 3 and 4 lead to the conclusion that these particles govern the observed differences in fatigue and propagation behavior. Now, concentrating on the fact that incoherent particles of different volume fraction and different sizes are present in the alloys, the following explanations are possible to describe the differences in fatigue crack propagation behavior.

In front of a propagating fatigue crack a plastic zone is formed. Within this plastic zone a displacement distribution is present with the greatest displacements directly ahead of the crack tip. The displacements decrease with increasing distance from the crack tip. Along the crack line, in the wake of the crack, high tensile plastic deformations remain when the crack propagates (7) (Fig. 6). The plastic displacements in front of the crack tip have a strong influence upon the build up of internal stresses, which together with the plastic displacements left behind the crack tip, lead to the crack closure behavior, which has a significant influence on crack propagation and retardation (8,9).

The amount of plastic displacement is dependent on the plastic deformation capability of the alloy. The plastic deformation capability can roughly be described by the strain to fracture or, better, by the potential for strain of the local elements ahead of the crack tip. In this connection the particle content of the alloy plays an important part. If an alloy has incoherent particles, the particles may crack or the particle matrix interface may fail during fatigue crack propagation; and voids are formed. Crack propagation by the coalescence of the voids is accompanied by extreme plastic deformation of the matrix. The stresses along the void contour become zero and a plane stress condition (10) develops locally; therefore, the matrix material between the particles show an extreme necking.

The influence of voids on the plastic deformation behavior has been discussed in the literature. In the case of the presence of voids, it was possible to show that the fracture strain ε_f, at which the voids coalesce, is higher in the direction parallel to the loading axis than in the direction transverse to the loading axis. McClintock (11) described the deformation parallel to the loading direction (first part of equation (1)) and Tracey (12) described the deformation transverse to the loading direction (second part of equation (1)).

$$\varepsilon_f = \ln \frac{l_t}{l_o} = -\frac{1}{\nu}\frac{l_p}{l_o} \qquad (1)$$

where l_o-spacing of the particles, l_t-longitudinal extension of the matrix, l_p-contraction of the matrix, ν-plastic Poisson's ratio. If now, for example, ε_f reaches the value of 0.7, the matrix extension is $2l_o$ parallel to the loading axis and 0.72 l_o transverse to the loading axis. The higher longitudinal elongation is visable in the form of sharp frames of the elongated dimple boundaries. It follows that the crack mechanism by the formation of voids is a highly deformation intensive mechanism. It occurs within the plastic zone

in front of the crack tip and dimples are left behind along the fracture surface during crack propagation. The high plastic displacements cause high residual stresses upon unloading. The crack surfaces come into contact early during unloading from the maximum load in a cycle (9). Early crack closure reduces the effective stress intensity and the crack propagation rates, especially in the retardation period after a high-low loading sequence.

The crack retardation of the particle rich technical alloys is more pronounced than the retardation of the particle free Al X-7075 alloy. The slip band type crack propagation mechanism of the Al X-7075 alloy does not allow such extremely high localized plastic deformations in front of and behind the crack tip.

The observed retardation in the tests increased as the crack grew larger. With increasing crack length and ΔK, a transition to the deformation rich dimple type crack propagation mechanism occurs. Up to now it was described that the existence of incoherent particles does influence the retardation behavior, but how can the differences be understood in retardation between the technical alloys Al 7075 and Al 7475?

Thomason (13) has shown the relation between the size and volume fraction of voids,

$$\varepsilon_f = \ln \frac{a}{T_0} \cdot Y \qquad (2)$$

where a is the diameter of the particles and Y is a factor considering the volume fraction of the particles. Based on this model Melander and Stählberg (14) could show that the size and distribution of voids has a considerable influence on ductile fracture. Two of their results, both of them important for the understanding of the differences in the deformation behavior of Al 7075 and Al 7475, will be referred to here.

- If there are particles of two sizes with a random distribution in the matrix, then the ductility increases when the width of the void size distribution increases. If there are small and large inclusions, the ductility is greater as if there are only inclusions of the same size.

- If there is a particle distribution such that between the large particles are a certain number of small ones, then the following happens:

  In the case where the volume fraction of small particles is larger than the volume fraction of the large particles (this is the case for Al 7475), the geometry of the small particles determines the critical strain. In this case, the deformations are relatively small.

  In the case where the volume fraction of the large particles is higher than that of the small particles (this is the case for Al 7075) then the ductility is governed by large voids. In this case, the deformations are relatively high.

Because there is a quite complicated algorithm behind these statements we refer to the original literature rather than showing the steps leading to these statements. Finally, it has to be taken into account that void formation around particles does not only occur in the plane of the later fracture surface, but additionally particles on either side in some distance of this plane contribute to the formation of voids (15).

In Fig. 7 the influence of the particles and their influence on the void formation is shown for different stages. Fig. 7a shows the distribution of particles for the example of two different sizes of inclusions. Fig. 7b shows that particles may brake or that the particle matrix interface fails and voids are formed. Failure and void formation do not only occur in the plane of final fracture but also in some distance on either side of the plane. This, together with the fact that the plastic displacements are dependent on the size distribution and volume fraction of the particles, will lead to high elongations of the material ahead of the crack tip and of the material in the wake of a propagating crack (Fig. 7c).

The amount of plastic elongation of the matrix between the voids is of some importance for the relevant crack closure displacements ahead of and behind the crack tip. It was also shown that the plastic elongations are greater when large and small particles are together than when only small ones are present. Compared with Al 7475, Al 7075 should show greater displacements (with a higher crack closure stress level), leading to more pronounced retardation in fatigue crack propagation after a high-low loading sequence.

The greater displacements ahead of the crack tip in Al 7075, as a result of the void formation, can only become effective in fatigue crack propagation tests with significant sequence effects, because void formation is a fatigue crack propagation mechanism only observed in the high loading regime. Here the fracture toughness of the alloy has a significant influence on the fatigue crack propagation behavior. In constant amplitude loading tests the low fracture toughness of Al 7075 dominates the fatigue cracks propagation behavior. Better results are obtained for Al 7475. After a high-low loading sequence, the fatigue crack propagation behavior at the low loading level is dominated by the actual displacement distribution and crack closure stress level. The result is a change in the fatigue crack propagation mechanism and a higher retardation in Al 7075 than in Al 7475.

SUMMARY

It was shown that the better retardation behavior of Al 7075, after a high-low loading sequence, compared to Al 7475 and the pure alloy Al X-7075 can be explained by the higher local displacements (displacements in the plastic zone ahead of the crack tip) because of incoherent particles which are sources of void formation during plastic deformation. The void formation results in higher plastic displacements dependent on size, distribution and volume fraction of the particles. Higher plastic displacements lead to an increase in the crack closure stress level and to a more pronounced retardation behavior.

ACKNOWLEDGEMENTS

The author wishes to thank Prof. Dr. W. W. Stinchcomb, Virginia Polytechnic Institute and State University, for the helpful discussion and for reading the manuscript. He also expresses his appreciation to Mrs. Marlene Taylor for typing the manuscript and Mr. G. K. McCauley for his assistance with the photo and art work.

REFERENCES

1. Sippel, K. O. and Weisgerber, D., 1975, ICAF 8th Congress Proceedings, Lausanne, Switzerland, pp. 7.1/1-7.1/55.

2. Nowack, H., Trautmann, K. H. and Hanschmann, D., 1979, ICAF 10th Congress Proceedings, Brussels, Belgium.

3. Buci, R. J., Thakker, A. B., Sanders, H. T., Sawtell, R. R. and Staley, J. T., 1980, ASTM STP 714, 41.

4. Staley, J. T., 1976, ASTM STP 605, 71.

5. Schulte, K., Trautmann, K. H. and Nowack, H., 1980, AEFM Conference Proceedings, Rome, Italy, 477.

6. Lowak, H., Franz, J. and Schütz, D., 1977, ICAF 5th Conference, ICAF Doc. No. 959, Darmstadt, W. Germany, 6/86.

7. Jacoby, G., Nowack, H. and Van Lipzig, H. T. M., 1976, ASTM STP 595, 172.

8. Elber, W., 1971, ASTM STP 486, 230.

9. Nowack, H., Trautmann, K. H., Schulte, K. and Lütjering, G., 1979, ASTM STP 677, 36.

10. Tetelman, A. S. and McEvily, A. S., "Fracture of Structural Materials", 1967, John Wiley & Sons, Inc., New York, USA.

11. McClintock, F. A., 1968, J. of Appl. Mechanics 35, 301.

12. Tracey, D. M., 1971, Eng. Fract. Mechanics 3, 301.

13. Thomason, P. F., 1968, J. of the Institute of Metals 96, 360.

14. Melander, A. and Ståhlberg, U., 1980, Int. Journ. of Fracture 16, 431.

15. Widgery, D. J. and Knott, J. F., 1978, Metal Science, 8.

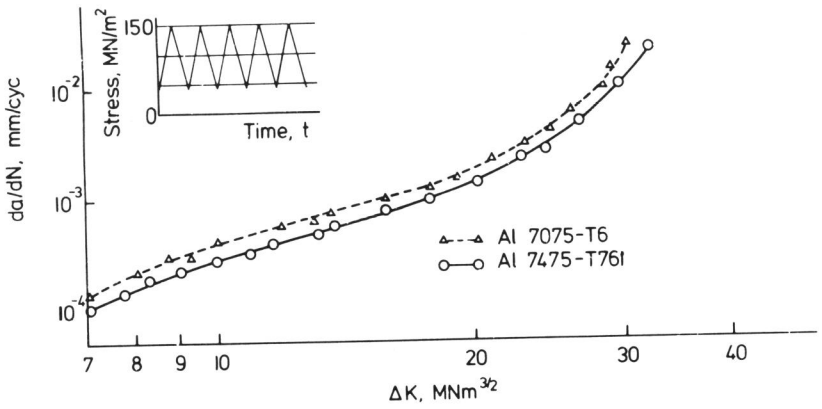

Fig. 1 Constant amplitude crack propagation behavior of 7075-T6 and 7475-T761 (R = 0.31)

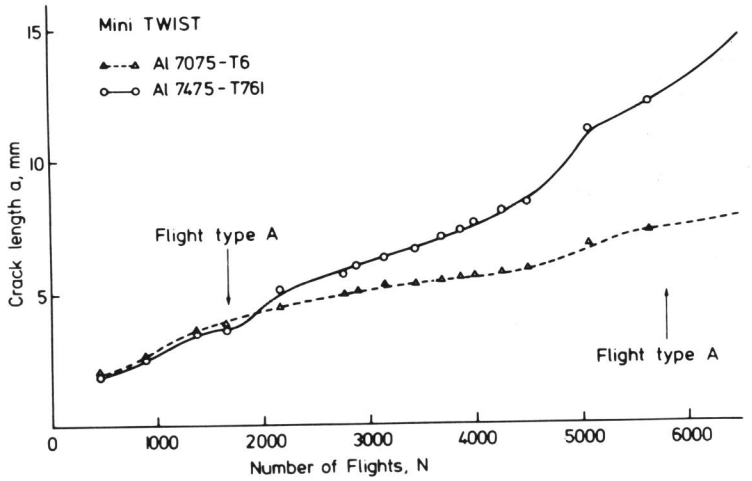

Fig. 2 Crack propagation behavior under Mini-TWIST loading

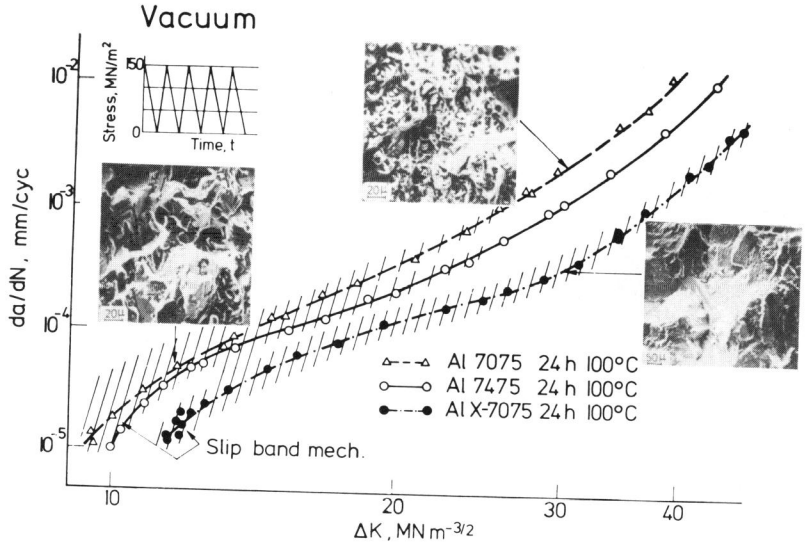

Fig. 3 Crack propagation behavior and microscopial crack propagation mechanism under constant amplitude loading

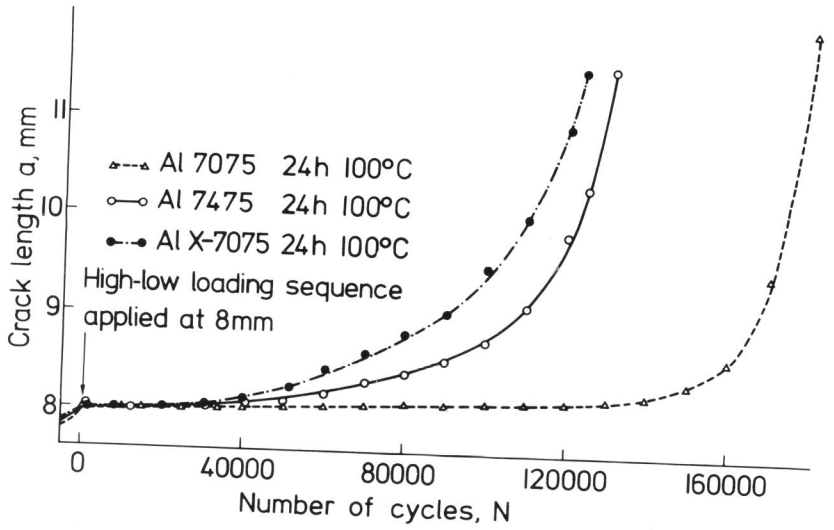

Fig. 4 Crack propagation behavior under a high-low loading sequence

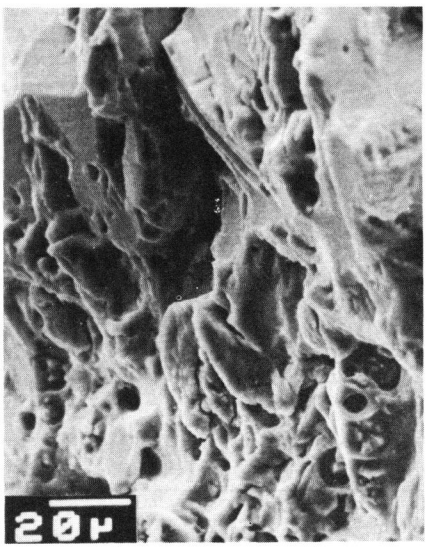

Fig. 5 SEM-micrograph, fracture surface Al 7075 24h 100°C, high-low loading sequence, transition region

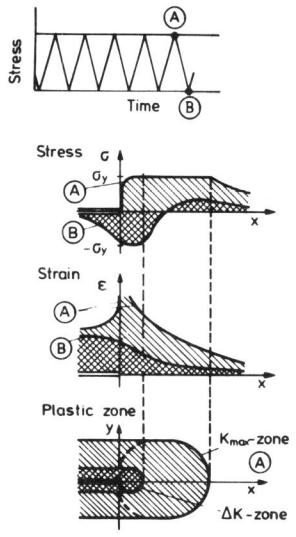

Fig. 6 Schemetical representation of stresses, strains and plastic zones in front of a propagating crack (7)

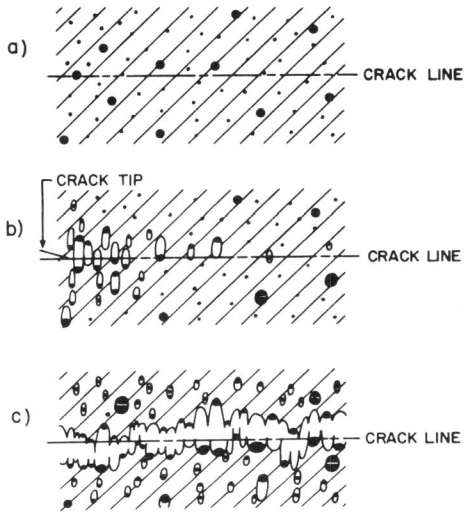

Fig. 7 Influence of particles to fracture process a) before fracture, b) ahead of crack tip, c) behind the crack tip